RSC Advances




ROYAL SOCIETY OF CHEMISTRY

www.rsc.org/advances

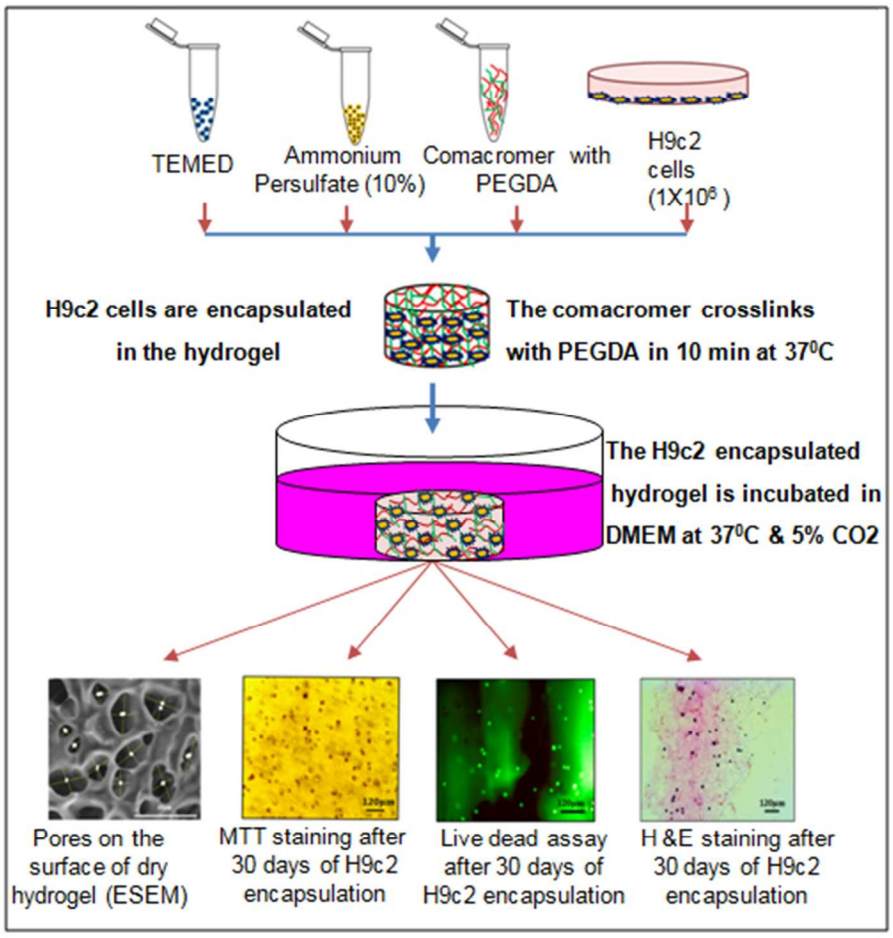


47x45mm (300 x 300 DPI)

Cite this: DOI: 10.1039/c0xx00000x

www.rsc.org/xxxxxx

ARTICLE TYPE

# Influence of matrix and bulk behaviour of injectable hydrogel on the survival of encapsulated cardiac cells

**Remya Komeri, Finosh Gnanaprakasam Thankam and Jayabalan Muthu ***

[a]Sree Chitra Tirunal Institute for Medical Sciences and Technology, Polymer Science Division, BMT Wing, Thiruvananthapuram – 695 012, Kerala State, India,

*Fax:0091-471-234814; Tel: 0091-471-2520212;E-Mail. mjayabalan52@gmail.com.

The cytocompatibility, suitable porosity, higher equilibrium water content and tissue like elasticity are the demanding criteria to design a hydrogel for cell encapsulation and delivery. Here a mechanically stable cell supporting synthetic hydrogel was fabricated from poly (propylene fumarate- co- ethylene glycol)/PEGDA by redox initiating polymerisation for cell encapsulation. A hydrogel prepared with 93.5% poly(propylene fumarate-co-ethylene glycol) and 6.5% PEGDA has acquired matrix and bulk characteristics of equilibrium water content (EWC) 84.45±0.80%, freezable water content 67.93%, Young modulus 212.2±0.02 kPa and pore diameter 88.64±18.96 µm. This hydrogel with higher free water content, favourable pore dimensions and mechanical strength was used to encapsulate cardiomyoblast. The encapsulated cardiomyoblast were showing increasing viability from 3-30 days with viable green fluorescence. The matrix and bulk characteristics of hydrogel are favourable and elicited uniform green fluorescing live cardiomyoblasts (H9c2) inside with 150% cell viability (MTT assay) and uniform ECM protein distribution after 30 days. The slow *in vitro* degradation of hydrogel in physiological-like conditions is favourable for delivery and retention of the encapsulated cells at the injection site.

Key words: Injectable hydrogel, matrix and bulk behaviour, encapsulated cardiac cells, longer survival

## Introduction

The population of cardiovascular disease (CVD) sufferers is drastically increasing during the recent years throughout the sphere. A statistical data from American Heart Association reported the occurrence of 1 death at every 40 seconds in USA due to CVD and 150000 silent deaths by myocardial infarction annually.[1] The myocardial infarction happens due to the ischemia of the ventricular wall by atherosclerotic or non-atherosclerotic (stress cardiomyopathy, cocaine ingestion, spontaneous coronary dissection, intense vaso constriction) reasons.[2] The reduced blood supply leads to the hypertrophy and necrosis of cardiomyocytes within 15 min.[3] The regenerative repair of infarct is challenging since the cardiomyocytes are terminally differentiated cells with a turnover ratio 1% per year.[4] The existing therapeutic interventions can reduce the oxygen consumption of remaining cardiomyocytes but not efficient to reduce the infarct size.[2] This may spread the ventricular remodeling to the non infracted area leads to wall thinning and cardiac rupture.

The cellular cardiomyoplasty is the practical choice for reducing the infarct size effectively. The cells are introduced by direct surgical intramyocardial injection, catheter based intramyocardial administration, trans endocardial injection, trans coronary venous injection, intravenous infusion and intracoronary artery administration.[5] But 90% of injected cells are lost in circulation and the remaining dies due to the harsh microenvironment.[5] These can be resolved by encapsulating the cells inside the *in situ* gelling injectable hydrogels.

The injectable hydrogels are well known for high tissue-like water content, limited surgical invasion and bulking effects.[6] The proper porosity (to promote immunoisolation and metabolite diffusion),[7] degradation proportional to allow the cell growth and moldability to fill the defective regions are some of the essential requirements for tissue engineering.[8] The hydrogels can be prepared from both natural and synthetic polymers by physical (poly electrolyte complexation, hydrogen bonding and hydrophobic association) or chemical (free radical polymerization, irradiation crosslinking) methods.[9] The hydrogels of decellularised porcine heart,[10] fibrin,[11] collagen,[12] matrigel,[13] chitosan,[14] and alginate[15] were developed for cardiomyoplasty. These biopolymers have excellent bioactive properties, but are poor in mechanical properties and biostability especially upon contact with body fluids. Risk of pathogen transfer, poor availability, cost, immunorejection and difficulty in purification are the major demerits of these natural polymers for cardiac applications.[9] Therefore the synthetic polymeric hydrogels are prefered for which the fine-tuning of mechanical, degradation properties and pore size are possible. The designing of synthetic hydrogels for efficient cell encapsulation is challenging due to the toxicity of leachables and poor cell adhesion. Poly (propylene fumarate) (PPF) is an interesting unsaturated linear polyester that degrades into fumaric acid and propylene glycol which are easily metabolisable. PPF contains crosslinkable double bonds which favours its application as *in situ* gelling injectable formulations. PPF has promise applications in cranio-facial bone implant due to its strength.[16] PEG, a FDA approved polyol imparts the hydrophilicity to the material.

PEG Diacrylate,[17] pHEMA-co-APMA grafted with

polyamidoamine hydrogel[18] and oligo (poly ethylene glycol fumarate) (OPF) hydrogels[19,20] were used to encapsulate different cell types. The fibroblast cells were encapsulated in PEG diacrylate based semi interpenetrating networks which were crosslinked with photopolymerisable I-2959.[17] But the hydrogel degrades completely within 32-35 days. The photopolymerisable pHEMA-co-APMA grafted with polyamidoamine hydrogel was reported with low swelling ratio; however it was not suitable for non-invasive *in vivo* applications due to poor light penetration.[18] The OPF hydrogels were used to encapsulate the bone marrow stem cells for cartilage tissue engineering[19] and embryonic stem cells for cardiac tissue engineering applications.[20] The OPF10K (PEG 9300 molecular weight) hydrogel with encapsulated embryonic stem cells was injected to the heart 1 week after MI.[20] The major drawback of OPF10K hydrogel was the higher degradation rate (completely degrades in 6 weeks).[21] The high swelling ratio of OPF10K decreased the mechanical strength (tensile modulus 16.5±4.6 kPa) and increased hydrolytic degradation.[21] The hydrogels with less degradation rate is desirable for cardiac applications. The mechanical support to the infracted myocardial wall for at least 5 months is essential to reduce the ventricular remodeling especially for infarct old enough to months.[6] With this background, we developed an injectable *in situ* gelling hydrogel of poly (propylene fumarate-co-ethylene glycol) crosslinked with PEGDA with very low degradation rate and required mechanical strength. The present paper deals with influence of physio chemical (presence of freezable and nonfreezable water), morphological (pore) and mechanical behaviour of injectable *in situ* gelling poly (propylene fumarate-co-ethylene glycol)/PEGDA hydrogel on the viability and proliferation of encapsulated cardiac cell.

## Results and Discussion

### Preparation of injectable formulation and hydrogels

The reaction scheme for the formation of poly(propylene fumarate-co-ethylene glycol)( CT PPF- PEG) comacromer and crosslinking with PEGDA to form hydrogel is narrated in Fig. 1. The hydrogels prepared by varying the ratio (%) of comacromer and PEGDA as 94.5: 5.5, 93.5: 6.5 and 92.5:7.5 were coded as PP5, PP6 and PP7 respectively. During the polyester formation, the cis-trans isomerization of maleic to fumaric acid is the decisive step which was accomplished by condensation reaction at high temperature. The ester bonds are formed by the carboxyl groups of fumarate and hydroxyl groups of propylene glycol to yield poly (propylene fumarate) with carboxyl termination.The comacromer is golden yellow with high viscosity. The crosslinking reaction with PEGDA is exothermic with negligible rise in temperature (Table 1), which may not affect the thermoregulation of body. The hydrogels sets at temperature less than 37 $^0$C within a reasonable period for injection (Table 1).

The functional groups of the CT PPF- PEG comacromer and the dried hydrogels were investigated with FT-IR spectral analyser. The FT-IR spectrum of the CT PPF- PEG crosslinkable comacromer (Fig. 2.1) shows the presence of a peak at 986.411 cm$^{-1}$ (CH bending of trans –CH=CH-) indicating the cis-trans isomerisation of maleic acid to fumaric acid during PPF synthesis as reported previously.[17] The peaks at 1642.09 cm$^{-1}$ (-C=C- stretching of –CH=CH- bond) indicates the successful condensation reaction with fumaric acid and 1, 2 propylene glycol to form PPF. The ester bond formation between the carboxyl group of PPF and hydroxyl group of PEG is indicated by the peak at 1723.09 cm$^{-1}$. The peaks at 3497.27 cm$^{-1}$ reveals the presence of hydroxyl groups of PEG in comacromer. The in situ gelling by crosslinking with comonomer was assessed by FT-IR spectral analyses of dry hydrogels (Fig. 2.2). The disappearance of peaks at 986.411 cm$^{-1}$ and 1642.09 cm$^{-1}$ in spectrum of hydrogels shows the crosslinking at the trans fumarate double bond in PPF by the crosslinker.

### Characterization of hydrogels

**Swelling and Crosslink density of hydrogels.** The physio chemical parameters of hydrogels are given in table 1. The equilibrium water content of PP5, PP6 and PP7 hydrogels are 85.72±0.53%, 84.45±0.80% and 82.76±0.52% respectively (Table 1). The proper diffusion of water is essential for the nutrient transport and metabolic waste exclusion for the cell survival inside the hydrogels. The hydrogel absorbs water until the free energy of mixing becomes equals to the elastic free energy of polymer network.[22] The swelling percentage depends on the degree of crosslinking, hydrophilicity of monomers, degree of neutralization of monomers and solvent interaction. Increasing the dilution and decreasing the crosslink density assist swelling.[22] The mobile ions inside the pores can further increase the osmosis. The ions create repulsive charges with the groups inside the pore and expand the coils to form large pores.[17] The neutralization and dilution of virgin CT PPF-PEG comacromer contributes more swelling ratio and higher equilibrium water content. The free sodium ions enhance the diffusion of solvent inside the hydrogel and create apt space for the cells. Chandy *et al* has reported 61.6±4.8% EWC for alginate/elastin/PEG hydrogel prepared for cell encapsulation.[23] Whereas the PP5, PP6 & PP7 hydrogels can hold more than 80% water (Table 1) highlight the suitability for tissue culture and cell encapsulation. The OPF-gelatin-added hydrogel[19] has been reported with very high swelling ratio of 13.9±0.2. Whereas the swelling ratio of the present PP5, PP6 & PP7 hydrogels are comparatively less for maintaining the proper mechanical stability and to prevent deformation after swelling (Table 1). The lower equilibrium water content (EWC) of PP7 hydrogel than the other hydrogels is due to the high crosslink density. The decrease in molecular weight between crosslinks for PP7 hydrogel shows the formation of closer crosslinking junctions.

**Mechanical property of hydrogels.** The compressive mechanical properties of hydrogels are given in the table 1. The mechanical forces of heart muscles are central to cardiac function throughout its contractile courses. The ventricular remodeling after myocardial infarction occurs to line up the mechanical force with ventricular wall thickness. The bulking effect of injectable hydrogel helps to maintain the mechanical property even after infarction. Kortsmit *et al* [24] studied the effect of hydrogel layers in infracted myocardial wall. If the stiffness of injected hydrogel is more than the surrounding myocardial tissue, the stress bearing capacity of wall increases. The stiffness of injectable hydrogel will reduce the remodeling or thinning of non-infracted myocardial wall. The myocardial stress of healthy control rat at end-diastole is 1.33 kPa and end systole is 13.33 kPa.[24] The PP5

hydrogel breaks at compressive stress of 7.76 kPa; it increases with increase in concentration of PEGDA (Table 1). The PP6 hydrogel has intermediate compressive stress of 24.48 kPa which is favourable for the cardiac application. The stiffness of hydrogel substrates influences the viability, morphology, and alignment of cardiac cells.[25] The Young modulus of PP5, PP6 & PP7 hydrogels are 68.8±0.043 kPa, 212.2±0.02 kPa and 258.7±0.05 kPa respectively (Table 1). The Young modulus of human myocardium is in the range of 20-500 kPa.[26] The Young moduli of PP5, PP6 and PP7 hydrogels falls in the range of native myocardium of human.

**Surface morphology and pore size of hydrogels.** The pore morphology on the surface of hydrogels is studied by ESEM micrographs. The pore length and width are measured by ImageJ software. Pore aspect ratio and diameter are measured as described by Dimonie *et al.*[27] The cell-cell contact and effective channeling of extracellular matrix proteins are necessary for the proper three dimensional cell growths. This necessitates the connection between the pores inside the hydrogel. The ESEM micrographs of PP5 (Fig. 3A), PP6 (Fig. 3B) and PP7 (Fig. 3C) hydrogels clearly shows interconnected pores. The alginate-elastin-PEG hydrogel for cardiomyoplasty was reported with 60-70 μm pore diameter.[23] The PP6 and PP5 hydrogels has 88.64±18.96 μm, 44.74±4.73 μm surface pore diameter respectively (Table 1). As reported by Venugopal *et al,* the pores of 50-100 μm allow vascularization.[26]

**Thermal property of hydrogels.** The nature of water present in the hydrogels is analysed by DSC thermogram (Fig. 3D). The nature of water inside the hydrogel influences the viability of encapsulated cells. The water in the hydrogels exist in three forms; Free water (FW) which undergoes similar phase transition on cooling or heating. Freezable bound water (FBW) weakly bound by the polymer interaction or capillary effect undergoes similar phase transition on cooling or heating. Whereas the strongly bound non-freezable bound water (NBW) is unable to undergo phase transition on cooling or heating. NBW is not detectable in differential scanning calorimetry (DSC).[28,29] The cooling curve in DSC displays the exothermic peak due to the crystallization of freezing water whereas the heating curve displays the endothermic peak due to the melting of frozen water in hydrogel (Fig. 3D). The freezable water content of PP5, PP6 and PP7 hydrogels is 74.43%, 68.14% and 67.93% respectively (Table 1). The remaining non-freezable bound water content is 11.30%, 16.52% and 14.62% for PP5, PP6 and PP7 hydrogels respectively. The poly vinyl alcohol-alginate IPN hydrogel has been reported previously with very low (5.165%) freezable water content.[28] The presence of higher percentage of freezable water in the present PP5, PP6 and PP7 hydrogels (Table 1) can significantly improve the nutrient and oxygen diffusion across the hydrogel. Even if the EWC of PP6 is higher than PP7, the non-freezable water content is more for PP6 (16.52%) which accounts for lower free water content comparable to other hydrogels. More than 50% free water content in these hydrogels is beneficial for the successful cell encapsulation and survival.

**In vitro degradation of hydrogels.** The in vitro degradation profile of hydrogels in physiological-like conditions was studied to ensure the required stability in biological fluid (Fig. 4). An ideal cell-encapsulated hydrogel must degrade proportional to the cell division and tissue formation. The hydrogels for cardiac cell delivery needs the slow degradation because the retention of mechanical property of hydrogel is necessary to reduce the ventricular remodeling in infarcted heart. In the first week the PP5, PP6 and PP7 hydrogels losses 0.3%, 0.35% and 0.5% by weight respectively in PBS whereas 0.5%, 0.55% and 0.15% by weight respectively in Ringer solution (Fig. 4A). The initial degradation of crosslinked junctions during the first week of encapsulation provides interconnected space for the viable cells to divide. The OPF hydrogels developed for embryonic stem cell transplantation by Wang *et al* degraded completely in 6 weeks.[20] The present PP5, PP6 and PP7 hydrogels undergo slow degradation proportional to the cell growth inside the hydrogel with only 0.2-0.6% weight loss even after 5 weeks (Fig. 4A). The degradation in PBS is slower than in Ringer's solution due to the presence of higher sodium ions in PBS than in Ringer. The higher sodium ion in incubation medium lowers the diffused water content in turn lowers the hydrolytic degradation rate. The increase in alkaline pH for PP5 and PP6 is comparable to the higher degradation rate in Ringer solution than PP7 (Fig. 4B). The pH variation is not significant from neutral pH in PBS due to the buffering action. The TDS variation depends on the charge of released products. The charged dissolved solids are responsible for the change in conductivity of the incubation medium (Fig. 4C & 4D). The variation in TDS and conductivity is not drastic due to the neutralization of the charged products released from the hydrogels in incubation medium.

**Studies on cytotocompatibility of hydrogels**

The cytotocompatibility of leachables and degradation products of hydrogels are investigated by MTT assay. The L929 monolayer shows 80% viability when incubated with 2.5 times diluted extract (Fig. 5). The degradation products from PP5, PP6 and PP7 also support the cell survival at 50% dilution (Fig. 5). The PP7 hydrogel extracts show comparatively higher viability in MTT assay (Fig.5.1). The higher crosslink density favours less release of leachables into the medium. The direct contact assay of PP5, PP6 and PP7 hydrogels on L929 monolayer does not change the spindle bipolarity of cells which reflects the cytocompatibility (Fig. 5B). Moreover the green fluorescing viable cells in live dead assay after direct contact test ensures the cell viability (Fig. 5C).

**Encapsulation of cardiomyoblast**

The nature of encapsulated cells largely depends on the bulk characteristics of the hydrogel substrates. In the present hydrogels systems, the spindle shaped cardiomyoblast in 2D culture appear in round morphology inside the hydrogel (Fig. 6A). Koh *et al* have also reported round morphology of 3T3 fibroblast encapsulated in PEG microgels.[30] The cell shape or polarity depends on the mechanical and physical characteristic of external microenvironment.[31] The cells can alter their morphology based on the shape of the lodging space in the matrix.[31] In 3D culture system (even in tissues), the cell-matrix interaction and the tension state decides the polarity of cells in the microtubule dependant or independent pathways. Rhee *et al* reported that the fibroblast cells under low tension retain the microtubule mediated cell shape including dendritic extensions, whereas higher tension

drive towards the circular morphology and loss of polarity.[32] The tension on cells inside the hydrogels is higher than in 2D culture which can drive the loss of extended cell morphology. The simultaneous cell extension by integrins on both dorsal and ventral sides and the extra mechanical intrusion by the external matrix are also responsible for the cell plasticity in 3D culture system.[32]

**Viability of encapsulated cardiomyoblast cells in hydrogels.** The viability of encapsulated cells in hydrogels was monitored after 3, 10, 20 and 30 days of encapsulation. The quantitative analysis of encapsulated cell viability was carried out using MTT assay. The cells in PP6 and PP7 hydrogels show increasing viability from 3 to 30 days of incubation (Fig. 6C). With OPF hydrogels, the rabbit marrow mesenchymal stem cell encapsulated-hydrogels were reported with decreasing proliferation of cells[19] from 0-28 days after encapsulation, whereas the viability of the encapsulated cells in the present hydrogels (PP5, PP6 & PP7) increases significantly from 3-30 days after encapsulation. The encapsulated cells in PP6 hydrogel show comparatively higher cell proliferation than PP5 & PP7. This can be explained by the favourable pore diameter, higher non-freezable water content and favourable mechanical strength of PP6 hydrogel than PP5 and PP7. A sudden decrease in cell viability is observed in PP5 hydrogel on 20$^{th}$ day. This is due to the increase in degradation and pH variation during 14- 20 days (Fig. 4A, 4B). The purple stained clusters of cells are present inside the MTT stained H9c2-encapsulated PP6 hydrogel even after 30 days (Fig. 6B). The viability of encapsulated cells in PP5, PP6 & PP7 hydrogels after 30 days is qualitatively reported by live/dead staining. The live /dead staining using acridine orange and ethidium bromide homodimer can stain necrotic and late apoptotic cells with lost membrane integrity in orange and live cells in green respectively. The green fluorescing viable, rounded H9c2 cells are observed in different plain inside the PP5, PP6 and PP7 hydrogels after 30 days of incubation (Fig. 7).

The Extracellular matrix proteins in cell encapsulated hydrogels after 30 days are qualitatively identified by H & E staining. The H9c2 cell encapsulated PP5, PP6 & PP7 hydrogels are stained with hematoxylin and counterstained with eosin. The hemalum binds DNA and stains nucleus blue, whereas eosin stains connective tissue, cytoplasm and other extracellular substances in various shades of pink.[33] The cells in PP5, PP6 & PP7 hydrogels are rounded in stained sections. The PP5 & PP6 hydrogels are uniformly stained in pink than PP7 hydrogel (Fig. 8). This shows an uniform distribution of extra cellular matrix proteins through the interconnected pores in the hydrogel necessary for cell- cell communication and division. These proteins can be secreted by the viable cells or adsorbed from the serum containing media on incubation.

## Experimental Section

### Synthesis of poly (propylene fumarate-co-ethylene glycol) comacromer

Carboxy terminated poly (propylene fumarate) (CT PPF) was synthesized by the esterification reaction between maleic acid and propylene glycol. Briefly, 1 M propylene glycol (M/S S.D. Fine chemicals) and 2 M maleic anhydride (MERK) was refluxed and condensed at 180 $^0$C for 2 h in nitrogen atmosphere. The reaction was catalyzed by morpholine and sodium acetate. The byproduct, water, was removed by applying vacuum for 20 min to inhibit the reverse reactions. The reaction product was then dissolved in acetone and precipitated with 25% aqueous methanol. The product was reprecipitated with petroleum ether to remove the unreacted low molecular weight reactants. Then filtered and dried at 60 $^0$C to get viscous and purified golden yellow resin. The purified poly (propylene fumarate) resin was condensed with poly ethylene glycol (300)( M/S Sigma Life Science) at 160 $^0$C for 45 min followed by vacuum condensation for 15 min to get the comacromer, poly (propylene fumarate-co-ethylene glycol) (CT PPF- PEG).

### FT-IR analyses of CT PPF- PEG

The structural characteristics of comacromer was identified by FT-IR spectrum recorded with FT-IR impact 410 spectrophotometer (Jasco, FT/IR-4200, USA) in the range of 4000-400 cm$^{-1}$ using JASCO's proprietary Spectra ManagerTM II software. A smear of resin was made over the glass slide and dried at 80 $^0$C for 2 days to remove moisture. The dried resin was dissolved in acetone and layered over the KBr pellet. The spectrum was corrected with spectra of acetone.

### Preparation of injectable formulation and hydrogel

The purified CT PPF- PEG comacromer was neutralized with sodium bicarbonate and diluted with PBS (4 ml/1g resin). The injectable formulation was prepared by blending the purified CT PPF- PEG comacromer with poly (ethylene glycol diacrylate) (PEGDA) (M/S Sigma Aldrich). Three hydrogels, PP5, PP6 and PP7 were prepared with ratio (%) of comacromer and PEGDA as 94.5: 5.5, 93.5: 6.5 and 92.5:7.5 respectively. The crosslinking was catalyzed by ammonium per sulfate (M/S Sigma Aldrich) and N, N, N', N'-tetra ethyl methyl ethylene diamine (TEMED). The hydrogels were prepared in a glass test tube using the initiator concentration as 10 µl of 10% APS and 1 µl of TEMED (6 M) per 200 µl neutralized resin. The setting time was monitored manually using a stopwatch at 37 $^0$C. The setting was confirmed by inverting the tube. The increase in temperature during setting was measured by a thermometer.

The hydrogels were casted in a plastic petri plate at 37$^0$C for 10 min using the above formulations. The hydrogels were washed with distilled water (DW) to remove the sodium bicarbonate crystals and leachables and freeze-dried (Christ Alpha 1-4 LD Freezedrier, UK) at 0.45 mbar pressure and -30$^0$C temperature. The freeze-dried hydrogel discs (10 mm in diameter, 3 mm in height) were used for the characterizations.

### Evaluation of Hydrogels

**Swelling percentage and equilibrium water content.** The freeze-dried hydrogel discs of known weights were soaked in 20 ml distilled water for 24 h at 37 $^0$C to achieve maximum swelling. The solvent on the surface of the swollen hydrogel was blotted softly and wet weight was measured. The weight-swelling ratio and equilibrium water content was calculated.[34] The equilibrium water content was calculated for the determination of non freezable water content. (DSC analysis).

**Crosslink density.** The crosslink density and number average

molecular weights between crosslinks were calculated for each hydrogels. The lyophilized circular hydrogels discs were swelled in different solvents (acetone, DMSO, methanol, ethanol, dimethyl acetamide and distilled water) for 48 h at 37 $^0$C. The swelling ratio in each solvent was calculated. The maximum swelling was observed in distilled water and the readings were used for calculating crosslink density. The diameter and thickness of circular hydrogel discs were measured using digital vernier calipers before and after swelling. Maximum swelling coefficient (Q) was calculated as the ratio of volume of the solvent in swollen material to that of the swelled material. The crosslink density was calculated from modified Flory-Rehner's equation.[35]

$$\text{Crosslink density } (\gamma) = -\frac{[\mathrm{Vr} + \chi \mathrm{Vr}^2 + \ln(1-\mathrm{Vr})}{\mathrm{drVo}\,(\sqrt[3]{\mathrm{Vr}} - \frac{\mathrm{Vr}}{2})}$$

Here $V_r$ is the volume fraction of the polymer in the swollen hydrogel equals to 1/1+Q. dr, the density of the polymer; $\chi$ , the polymer lattice interaction parameter (0.34 for the maximum swelling) and $V_0$ , the molar volume of the solvent. The number average molecular weight between crosslinks ($M_C$) was calculated as the reciprocal of crosslink density (mol/cm$^3$).

**Determination of mechanical property.** The PP5, PP6 and PP7 hydrogel samples (1 cm height and 1 cm diameter) were prepared in a cylindrical mold. The samples were swelled in PBS for 24 h. The height and diameter was measured after swelling using digital vernier calipers. The unconfined Young modulus was identified using Instron compression instrument 3345 (Bioplus, India) with wide compression probe. The hydrogels were compressed to 60% of the original height at the rate of 5 mm/min with 500 N load cell at RT. The compressive stress at maximum load and Young modulus were measured using the bluehill 3.13 software.

**Surface pores on hydrogel.** The surface morphology and pore distributions of the hydrogels (swelled) were analysed by electron microscopy (ESEM, FEI, Quanta 200, USA). The freeze-dried hydrogels were swelled in distilled water to enhance the visibility of pores on the surface. The swelled hydrogels maintained the pores as such without cracking. The image J software was used to measure the pore length and width. The longest distance across the pore is the length (L) and longest distance perpendicular to the length is width (W). The pore diameter (D) was calculated as $\sqrt{L \times W}$.[27] The aspect ratio (A) of pores was calculated as $L/W$. The pore aspect ratio of spherical or rectangular pores is in between 1 to 1.5, elliptical pores in 1.5 to 3.5.

**Thermal analysis of hydrogel.** The phase transition of water in hydrogel material was studied using differential scanning calorimetry (DSC Q20 V24.4 Build 116, TA Instruments). The lyophilized PP5, PP6 and PP7 hydrogels were swelled in distilled water (DW) for 24 h. 5 mg of sample was cooled to **(-)** 60 $^0$C and gradually heated to 100 $^0$C at a rate of 5 $^0$C/min in nitrogen atmosphere. The thermogram was scanned from -80 $^0$C to 100 $^0$C with heating rate of 5 $^0$C/ min in nitrogen atmosphere using an empty aluminium pan as reference. The freezable water content ($W_f$) was calculated as the ratio of endothermic heat flow of hydrogel to the endothermic heat flow of pure water (334 J/g). The non freezable water content ($W_{nf}$) was given by subtracting the free water content from equilibrium water content.

**In vitro degradation of hydrogel.** The lyophilized hydrogels (10 mm in diameter, 3 mm in height) were weighed and subjected to aging in 20 ml PBS and Ringer solution at 37 $^0$C (in physiological-like conditions) in an orbitol shaker. The remaining dry weights of hydrogels were measured after 7, 14, 21, 28 and 35 days of incubation. 5 ml incubation medium was added to maintain the fluid level to 20 ml after each 5 days. The pH, total dissolved solids and conductivity of the incubation medium after 7, 14, 21, 28 and 35 days were recorded with pH meter connected to conductivity probe (Cyberscan pH 510, Eutech instruments).

### Cytocompatibility of hydrogels

The cytocompatibility of hydrogels was evaluated on L929, rat fibroblast monolayer (NCCS, Pune). The cells were cultured in Delbecco's modified eagles medium containing high glucose (DMEM, Gibco, USA) supplemented with 0.37% sodium bicarbonate (M/S Sigma, USA), 10% Fetal bovine serum (South American origin, Gibco, USA ) and 1% antibiotic-antimycotic solution (Gibco, USA). Cells were cultured at 37 $^0$C and 5% $CO_2$ in a humidified incubator.

**Cytotocompatibility of leachable from hydrogels.** The neutralized diluted resin with 5%, 6%, 7% PEGDA and initiator were filtered through 0.22 µm cellulose acetate filter. The hydrogel samples were prepared in 24 well plates and incubated in 1 ml DMEM media for 72 h at 37 $^0$C. The media containing the leachable was used for viability testing on L929 mouse fibroblast cells. Around 5x10$^3$ cells were seeded in the 24 well plate to reach 70% confluent. The extracted media was diluted 0.5 and 2.5 times with fresh DMEM media. The cells were incubated for 24 h at 37 $^0$C and 5% $CO_2$. Each sample was taken in triplicates. The culture media was removed and washed with PBS. The cells were incubated with 50 µl MTT solution (5 mg/ml in PBS) per well for 4 h at 37 $^0$C. The formazan crystals were extracted on 200 µl DMSO for 30 min at room temperature. The absorbance was measured at 540 nm using ASYS UVM 340 plate reader.

**Cytotoxicity of degradation products from hydrogels.** The hydrogels in 20 ml Ringer solution were kept in orbital shaker for 35 days to allow degradation. The Ringer solution containing the degraded fractions was collected after 35 days and lyophilized. The lyophilized powder was resuspended in 10 ml DMEM medium and filtered. The monolayer of L929 cells were incubated with the 1:1 mixture of degradation media and fresh DMEM media for 24 h at 37 $^0$C. The MTT assay was conducted as given before and the viability was calculated.

**Direct contact on L929 monolayer.** L929 cells (1x10$^4$) were seeded in 96 well plate and cultured till 80% confluency. 10 mg of PP6 hydrogels were incubated with L929 cells for 24 h at 37 $^0$C. The micrographs were taken to assess the morphology of the cells. The live cells were identified by live dead staining. The cells were washed with PBS once and stained with 5 µg of acridine orange and 5 µg of ethidium bromide in PBS. Excess stain was washed with PBS. Images were taken using epiflourescence microscope (Optika, Italy).

### Encapsulation of cardiomyoblasts in hydrogels

The H9c2 cardiomyoblast cells were encapsulated in PP5, PP6 and PP7 hydrogels. H9c2 cells were grown in high glucose

DMEM media with 1.5 g/L sodium bicarbonate, 10% FBS and 1% antimycotic solution. The cells were trypsinized and centrifuged at 3000 rpm to the cell pellet. The cells were counted using hemacytometer. Around 1x $10^6$ cells were dispensed in neutralized CT PPF- PEG comacromer – PEGDA suspension. The cells were encapsulated within 10 min after the addition of 10 µl APS (10%) and 1 µl TEMED. The H9c2 cell encapsulated gels were incubated in 1 ml DMEM media in 24 well plate. The media was changed in every alternate day.

**Live dead assay for encapsulated cells.** The H9c2 cell encapsulated hydrogels after 35 days were washed with PBS. Equal volumes of 100 µg/ml acridine orange and 100 µg/ml ethidium bromide homodimer were mixed. 20 µl from the mixture was directly added to the hydrogel. Incubated for 5 min and washed with PBS twice. The photographs were taken using epifluorescence microscope (Optika SRL, Italy) in green and red filter and the images were merged.

**MTT staining & viability assay for encapsulated hydrogels.** The H9c2-encapsulated hydrogels after 3, 10, 20 and 30 days were washed with PBS. 1 ml serum free DMEM media with 1 mg/ml MTT solution was added to each gel. The hydrogels were incubated overnight at 37 $^0$C and 5% $CO_2$. The micrographs were taken to visualize the live encapsulated cells. Then the hydrogels were vortexed and broken in 1 ml DMSO for 2 h at room temperature. The gels were centrifuged, collected the supernatant and measured the absorbance at 540 nm. The absorbance of blank hydrogels (hydrogels without encapsulation but incubated with 1 mg/ml MTT in DMEM) were substracted from the test samples. The viability percentage was measured against the control cells of 3, 10, 20 and 30 days after seeding.

**Hematoxylin & eosin staining of encapsulated hydrogels.** The H9c2 cell encapsulated hydrogels after 34 days were embedded in tissue freezing medium (Jung, Germany). The cryo sections of 10 µm thickness were taken using LEICA CM 3050S microtome. The sections were stained with hematoxylin stain (M/S HIMEDIA) for 2 min, washed under tap water for 2 min, destained with acid alcohol until the sections looks red and washed under tap water. The slides were dipped in bluing solution for 2 min and thoroughly rinsed with tap water. The slides were rinsed in 95% ethanol followed by eosin (M/S HIMEDIA) counterstaining for 30 sec. The slides were dehydrated by dipping in 70, 80, 95 and 100% ethanol each step with 2-3 min. The photographs were taken in phase contrast microscope after 10 min.

## Conclusion

The present chemically crosslinked hydrogels from poly (propylene fumarate-co-ethylene glycol) / PEGDA hold more than 80% water inside the hydrogel with the required mechanical property. The higher freezable water content and interconnected porosity of PP6 hydrogel accounts for the successful cell encapsulation. The Young moduli of the hydrogels are comparable to the human myocardial tissue. The PP6 hydrogel shows significant proliferation of encapsulated cells till 30 days after encapsulation. The cells inside the hydrogel reach the viability greater than 2D control within 30 days after encapsulation in *in vitro* culture. Moreover, the slow degradation adds to the maximum cell retention and proliferation. Therefore the present synthetic, in situ gelling, injectable, mechanically stable, cell supporting hydrogel of poly (propylene fumarate-co-ethylene glycol) with 6% PEGDA have favourable matrix and bulk properties for successful cardiac cell encapsulation and delivery.

## Statistical analysis

All experiments were performed at least 3 times and the data were reported as mean ± standard deviation using Microsoft Office Excel 2007. The significance in difference was analysed by students t test using GraphPad QuickCals online t test calculator. The values of $p < 0.05$ were considered significant

## Acknowledgments

The authors thank The Director and Head, BMT Wing, SCTIMST for providing the facilities to carry out this work. The authors acknowledge the help provided by Vineeth.V.M, Dr. Sunitha Prem Victor and Dr. Shivaram Selvan during the studies. R.K. acknowledges the financial support from CSIR, New Delhi, Government of India for Junior Research Fellowship (2014-2015).

## Notes and references

1 A. S. Go, D. Mozaffarian, V. L. Roger, E. J. Benjamin, M. B. Turner and on behalf of the American Heart Association Statistics Committee and Stroke Statistics Subcommittee, *Circulation*, 2014, **129**, e28–e292.

2 V. Soukoulis, W. E. Boden, S. C. Smith and P. T. O'Gara, *Circ. Res.*, 2014, **114**, 1944-1958.

3 J. S. Alpert, K. Thygesen , E. Antman , J. P. Bassand, *J Am Coll Cardiol.*, 2000, **36**, 959-69.

4 P. W. Burridge, G. Keller, J. D. Gold and J. C. Wu, *Cell Stem Cell*, 2012, **10**, 16-28.

5 C. C. Sheng, L. Zhou and J. Hao, *BioMed Res. Int.*, 2012, **2013**, e547902.

6 E. Tous, B. Purcell, J. L. Ifkovits and J. A. Burdick, *J Cardiovasc. Transl. Res.*, 2011, **4**, 528-542.

7 X. Tang, P. Bajaj, R. Bashir and T. A. Saif, *Soft Matter*, 2011, **7**, 6151.

8 D. J. Overstreet, D. Dutta, S. E. Stabenfeldt and B. L. Vernon, *J. Polym. Sci. Part B Polym. Phys.*, 2012, **50**, 881-903.

9 I. M. El-Sherbiny and M. H. Yacoub, *Glob. Cardiol. Sci. Pract.*, 2013, **2013**, 316–342.

10 J. M. Singelyn, J. A. DeQuach, S. B. Seif-Naraghi, R. B. Littlefield, P. J. Schup-Magoffin and K. L. Christman, *Biomaterials*, 2009, **30**, 5409-5416.

11 Q. Ye, G. Zünd, P. Benedikt, S. Jockenhoevel, S. P. Hoerstrup, S. Sakyama, J. A. Hubbell and M. Turina, *Eur. J. Cardio-Thorac. Surg. Off. J. Eur. Assoc. Cardio-Thorac. Surg.*, 2000, **17**, 587-591.

12 I. Kutschka, I. Y. Chen, T. Kofidis, T. Arai, G. von Degenfeld, A. Y. Sheikh, S. L. Hendry, J. Pearl, G. Hoyt, R. Sista, P. C. Yang, H. M. Blau, S. S. Gambhir and R. C. Robbins, *Circulation*, 2006, **114**, I167-173.

13 L. Ou, W. Li, Y. Zhang, W. Wang, J. Liu, H. Sorg, D. Furlani, R. Gäbel, P. Mark, C. Klopsch, L. Wang, K. Lützow, A. Lendlein, K. Wagner, D. Klee, A. Liebold, R.-K. Li, D. Kong, G. Steinhoff and N. Ma, *J. Cell. Mol. Med.*, 2011, **15**, 1310-1318.

14 H. Wang, X. Zhang, Y. Li, Y. Ma, Y. Zhang, Z. Liu, J. Zhou, Q. Lin, Y. Wang, C. Duan and C. Wang, *J. Heart Lung Transplant. Off. Publ. Int. Soc. Heart Transplant.*, 2010, **29**, 881-887.

15 O. Tsur-Gang, E. Ruvinov, N. Landa, R. Holbova, M. S. Feinberg, J. Leor and S. Cohen, *Biomaterials*, 2009, **30**, 189-195.

16 A. M. Henslee, D. M. Yoon, B. Y. Lu, J. Yu, A. A. Arango, L. P. Marruffo, L. Seng, T. D. Anver, H. Ather, M. B. Nair, S. O. Piper, N.

Demian, M. E. K. Wong, F. K. Kasper and A. G. Mikos, *J. Biomed. Mater. Res. B Appl. Biomater.*, 2014, n/a–n/a.
17 J. K. Kutty, E. Cho, J. Soo Lee, N. R. Vyavahare and K. Webb, *Biomaterials*, 2007, **28**, 4928-4938.
18 D. Kumar, I. Gerges, M. Tamplenizza, C. Lenardi, N. R. Forsyth and Y. Liu, *Acta Biomater.*, 2014, **10**, 3463-3474.
19 H. Park, X. Guo, J. S. Temenoff, Y. Tabata, A. I. Caplan, F. K. Kasper and A. G. Mikos, *Biomacromolecules*, 2009, **10**, 541-546.
20 H. Wang, Z. Liu, D. Li, X. Guo, F. K. Kasper, C. Duan, J. Zhou, A. G. Mikos and C. Wang, *J. Cell. Mol. Med.*, 2012, **16**, 1310-1320.
21 J. S. Temenoff, K. A. Athanasiou, R. G. Lebaron and A. G. Mikos, *J. Biomed. Mater. Res.*, 2002, **59**, 429-437.
22 S. V.-F. Fariba Ganji, *Iran. Polym. J.*, 2010, **19**, 375-398.
23 T. Chandy, G. H. R. Rao, R. F. Wilson and G. S. Das, *J. Biomater. Appl.*, 2003, **17**, 287-301.
24 J. Kortsmit, N. H. Davies, R. Miller, J. R. Macadangdang, P. Zilla and T. Franz, *Comput. Methods Biomech. Biomed. Engin.*, 2013, **16**, 1185-1195.
25 S. Al-Haque, J. W. Miklas, N. Feric, L. L. Y. Chiu, W. L. K. Chen, C. A. Simmons and M. Radisic, *Macromol. Biosci.*, 2012, **12**, 1342-1353.
26 J. R. Venugopal, M. P. Prabhakaran, S. Mukherjee, R. Ravichandran, K. Dan and S. Ramakrishna, *J. R. Soc. Interface*, 2012, **9**, 1-19.
27 D. Dimonie, M. Petrache, R. Trusca, E. Vasile, S. M. Dinescu, R. C. Fierascu, *Dig. J. Nanomater. Biostructures*, 2013, **8**, 11-24
28 F. Gnanaprakasam Thankam, J. Muthu, V. Sankar and R. Kozhiparambil Gopal, *Colloids Surf. B Biointerfaces*, 2013, **107**, 137-145.
29 F. G. Thankam and J. Muthu, *J. Bioact. Compat. Polym.*, 2013, **28**, 557-573.
30 W.G. Koh, A. Revzin and M. V. Pishko, *Langmuir ACS J. Surf. Colloids*, 2002, **18**, 2459-2462.
31 C. Moraes, B. C. Kim, X. Zhu, K. L. Mills, A. R. Dixon, M. D. Thouless and S. Takayama, *Lab. Chip*, 2014, **14**, 2191-201.
32 S. Rhee, H. Jiang, C.-H. Ho and F. Grinnell, *Proc. Natl. Acad. Sci. U. S. A.*, 2007, **104**, 5425-5430.
33 V. Keskar, N. W. Marion, J. J. Mao and R. A. Gemeinhart, *Tissue Eng. Part A*, 2009, **15**, 1695-1707.
34 F. G. Thankam and J. Muthu, J Biomed Mater Res Part A. 2013, 00A: 000–000.
35 M. Jayabalan, P. P. Lizymol and V. Thomas, *Polym. Int.*, 2000, **49**, 88–92.

Figure captions

Figure 1: Schematic representation of synthesis of carboxy terminated poly (propylene fumarate -co-ethylene glycol) comacromer and hydrogel.

Figure 2: FT-IR spectra of CT PPF- PEG comacromer and hydrogels. CT PPF- PEG comacromer (2.1). PP5 (2.2A), PP6 (2.2B) and PP7 (2.2C).

Figure 3: The ESEM micrographs of hydrogels. PP5 (A), PP6 (B), PP7 (C) and the representative DSC thermogram of PP6 hydrogel (D).

Figure 4: In vitro degradation profile of hydrogels in PBS and Ringer incubation medium. Weight loss (%) (A), pH variation (B), TDS variation(C) and conductivity variation (D).

Figure 5: Cytocompatibility of leachables and degradation products of hydrogels. MTT assay of leachables (5.1). Cell survival assy of degradation products (5.2), L929 control cells (A), direct contact test for PP6 hydrogel (B) and live dead assay after direct contact test for PP6 hydrogel(C).

Figure 6: The viability of encapsulated cardiomyoblast in hydrogels. Cardiomyoblast encapsulated in PP6 hydrogel (A), MTT stained viable cells inside PP6 hydrogel (B), cell viability of encapsulated cardiomyoblast after 3, 10, 20 and 30 days inside PP5, PP6 and PP7 hydrogels (C).

Figure 7: Live dead assay of cardiomyoblast encapsulated in hydrogels, PP5 (A), PP6 (B) and PP7 (C).

Figure 8: H & E staining of cardiomyoblast encapsulated in hydrogels, PP5 (A), PP6 (B) and PP7 (C).

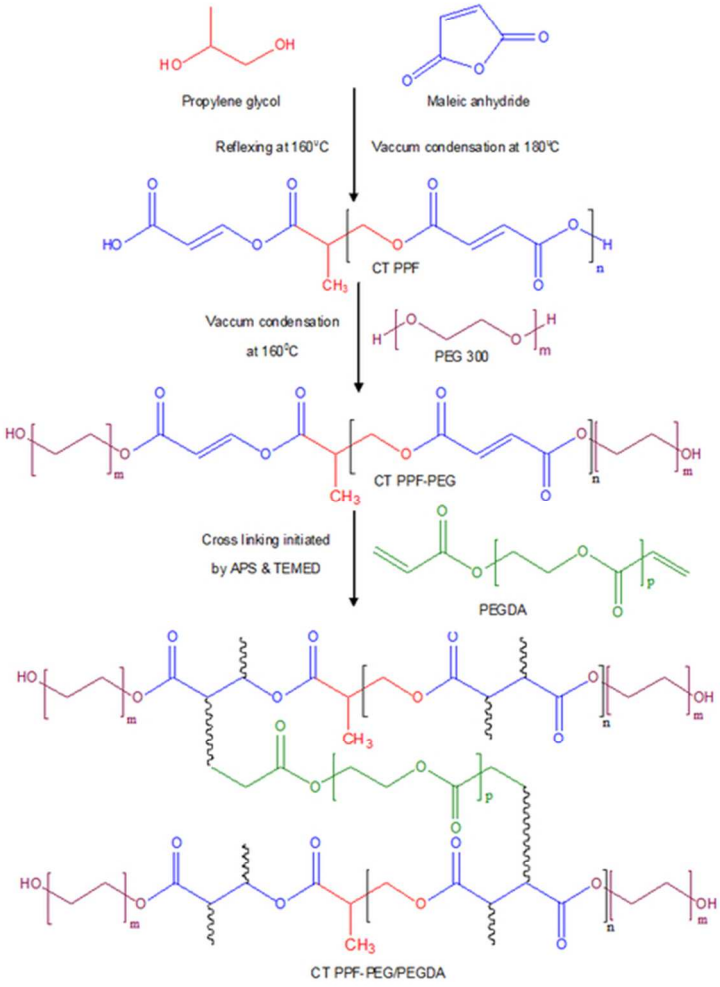


Figure 1
24x35mm (600 x 600 DPI)

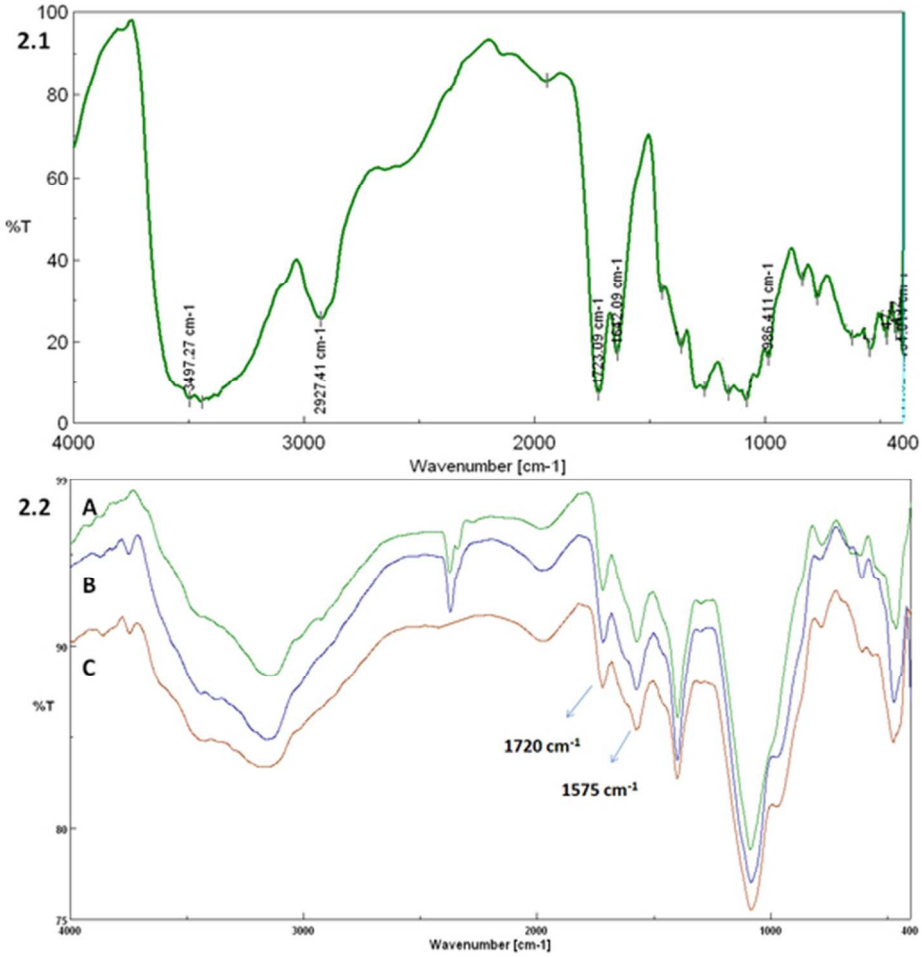


Figure 2
26x25mm (600 x 600 DPI)

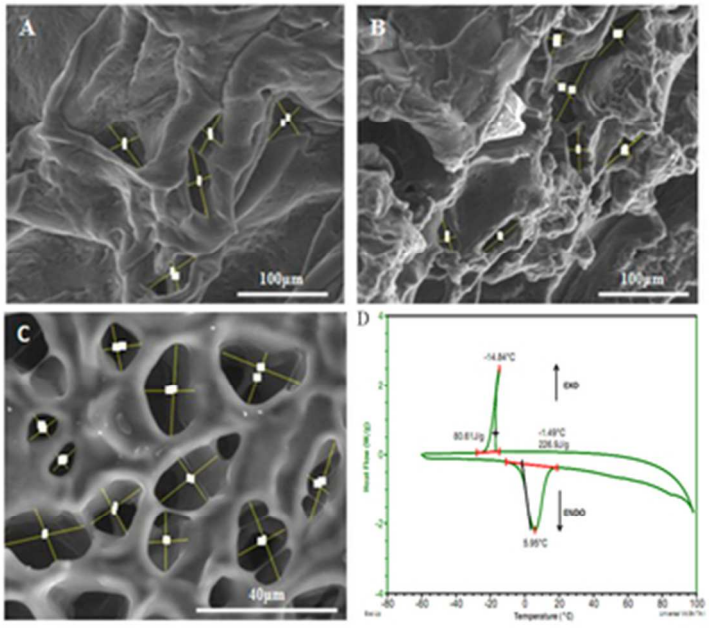


Figure 3
31x27mm (300 x 300 DPI)

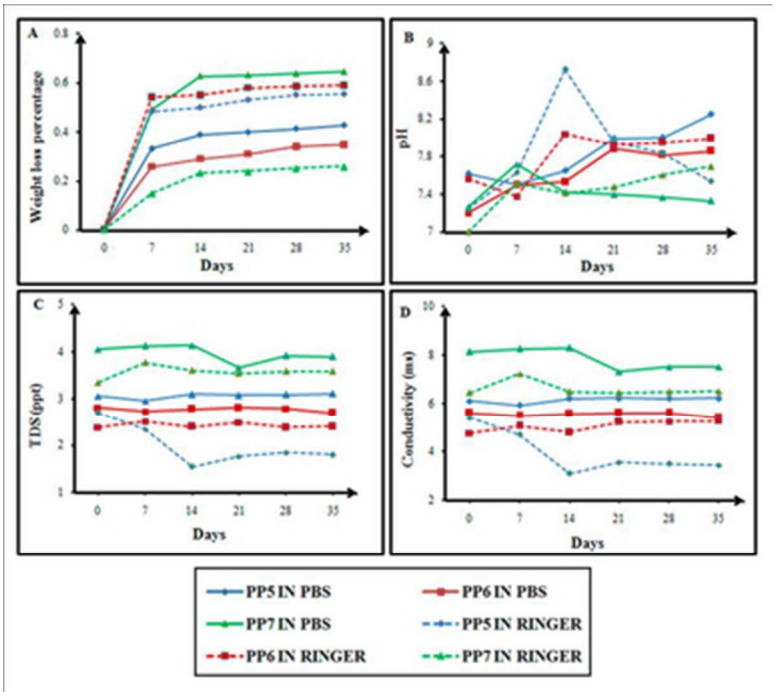


Figure 4
32x29mm (300 x 300 DPI)

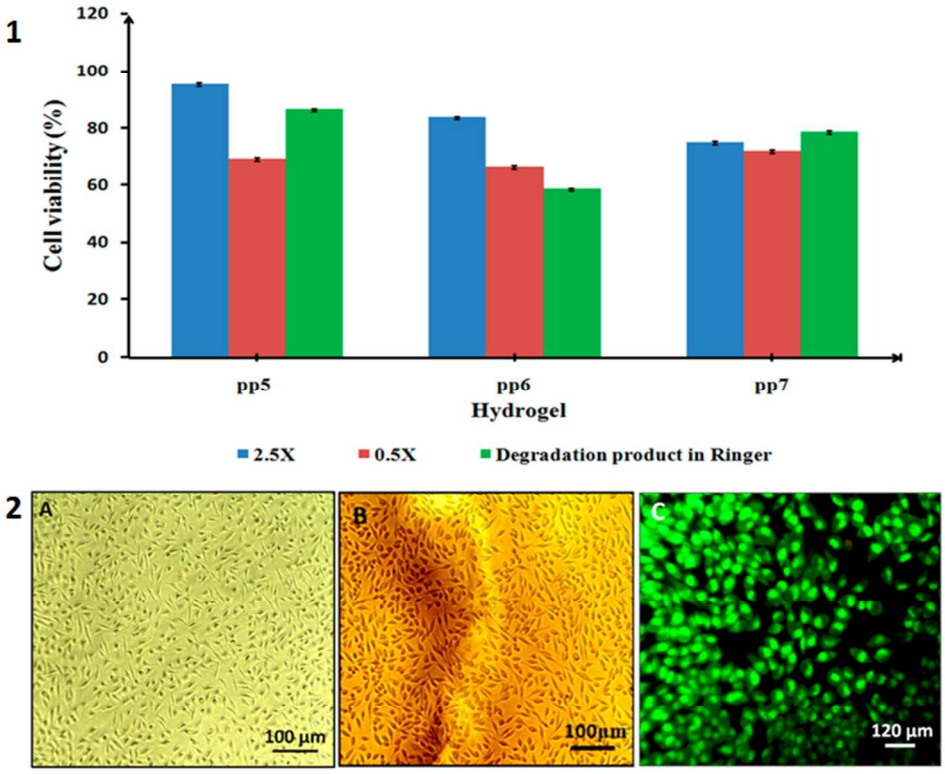


Figure 5
277x234mm (72 x 72 DPI)

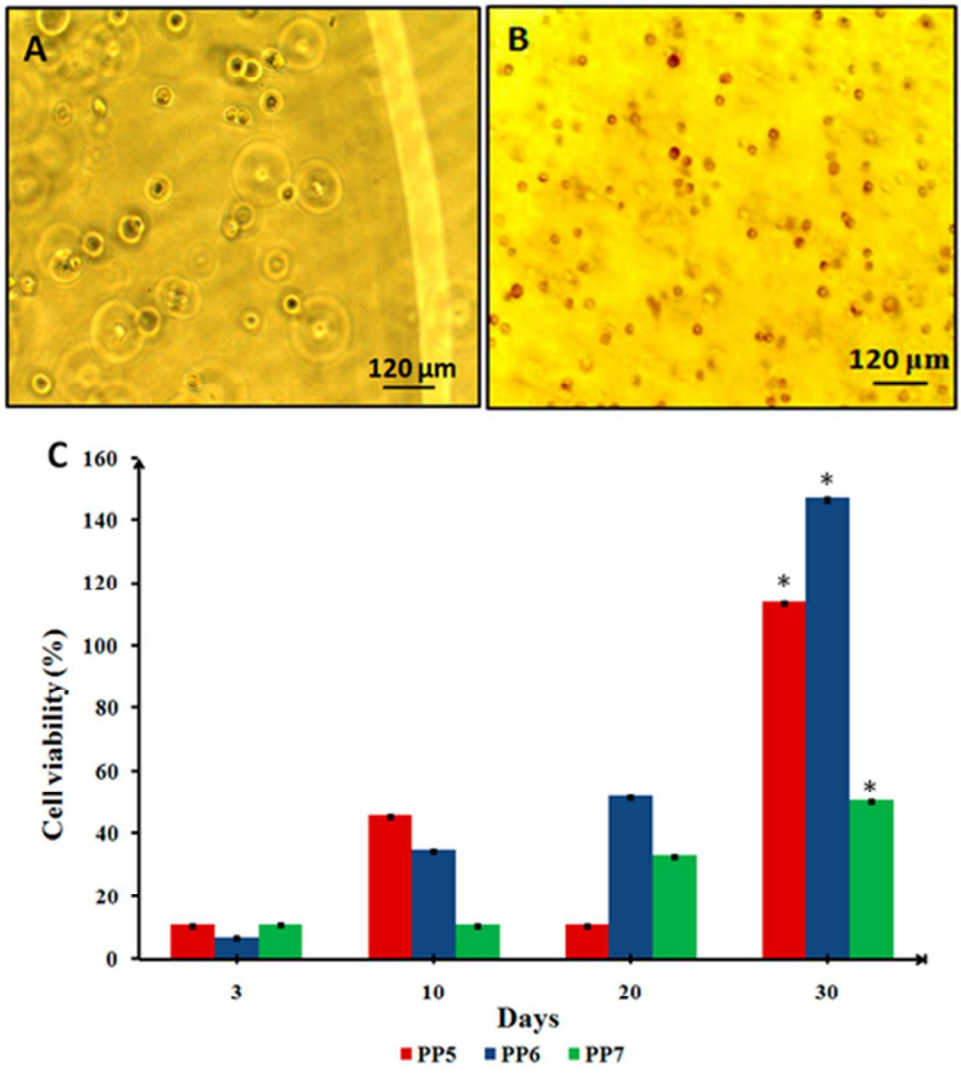


Figure 6
44x49mm (300 x 300 DPI)

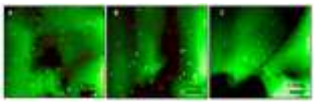

Figure 7
13x4mm (300 x 300 DPI)

Figure 8
14x4mm (300 x 300 DPI)

**Table 1 :Physio chemical, mechanical and thermal properties of PP5, PP6 and PP7 hydrogels**

| Properties | PP5 | PP6 | PP7 |
|---|---|---|---|
| **1.Setting characterestics** | | | |
| Setting temperature($^0$C) | 33.5 | 33.5 | 33 |
| Rise in temperature during setting ($^0$C) | 1.5 | 2 | 2 |
| Setting time (min) | 12 | 10 | 9 |
| **2.Swelling properties** | | | |
| Weight swelling ratio | 7.01 ± 0.27 | 6.44 ± 0.34 | 5.58 ± 0.17 |
| Equilibrium water content (%) | 85.72 ± 0.53 | 84.45 ± 0.80 | 82.76 ± 0.52 |
| Cross linking density (mol/cm$^3$) | 0.023 ± 0.002 | 0.024 ± 0.003 | 0.027 ± 0.005 |
| Molecular weights between Crosslinks (g/cm$^{3)}$) | 42.82 ± 4.79 | 38.41 ± 6.94 | 37.20 ± 8.12 |
| **3.Mechanical properties** | | | |
| Maximum load(N) at break | 0.626 ± 0.403 | 1.7691 ± 0.17 | 2.3876 ± 0.26 |
| Youngs modulus (kPa) | 68.8 ± 0.043 | 212.2 ± 0.02 | 258.7 ± 0.05 |
| Compressive stress (kPa) | 7.7 ± 0.004 | 24.4 ± 0.003 | 31.6 ± 0.002 |
| **4.Thermal analysis** | | | |
| Onset of $T_{endo}$ | -1.68 | -1.49 | -1.45 |
| Enthalpy of melting of freezing water (Jg−1) | 248.6 | 226.9 | 227.6 |
| Onset of crystallizationof freezing water (◦C) | -18.98 | -17.06 | -19.79 |
| Enthalpy of crystallization of freezing water (J g−1) | 153.4 | 80.61 | 117.7 |
| Freezable free water content (%) | 74.43 | 67.93 | 68.14 |
| Non-freezable water content (%) | 11.30 | 16.52 | 14.62 |
| **5.Porosity** | | | |
| Pore aspect ratio | 1.91 | 1.80 | 1.58 |
| Pore diameter (μm) | 44.74 ± 4.63 | 88.64 ± 18.96 | 16.40 ± 2.86 |
| Shape of the pore | Elliptical | Rectangular | Almost spherical |